Supplement of The Cryosphere, 14, 4603–4609, 2020
https://doi.org/10.5194/tc-14-4603-2020-supplement

The Cryosphere
Open Access

Supplement of

Brief communication: Heterogenous thinning and subglacial lake activity on Thwaites Glacier, West Antarctica

Andrew O. Hoffman et al.

Correspondence to: Andrew O. Hoffman (hoffmaao@uw.edu) and Knut Christianson (knut@uw.edu)

1 Introduction

Here we provide additional information on the glaciostatic hydropotential time series, water routing, and describe the diagnostic model simulations we use to interrogate the influence of lake fill-drain cycles on basal resistance and ice sliding velocity.

2 Lake volume change

We applied the same SAR LOS methods to measure vertical displacements on the lakes identified by Smith et al. (2017) to estimate lake volume change on the lakes identified in the western Haynes Glacier shear margin (Fig. S1). We also created average lake volume change estimates from the gridded CryoSat-2 time series (Fig. S2). We note that ice velocity changes are not detectable in SAR data outside of lake polygons (Fig. S3). This suggests that the velocity signals observed with GNSS are below the detection threshold of the SAR data and/or very spatially limited in extent.

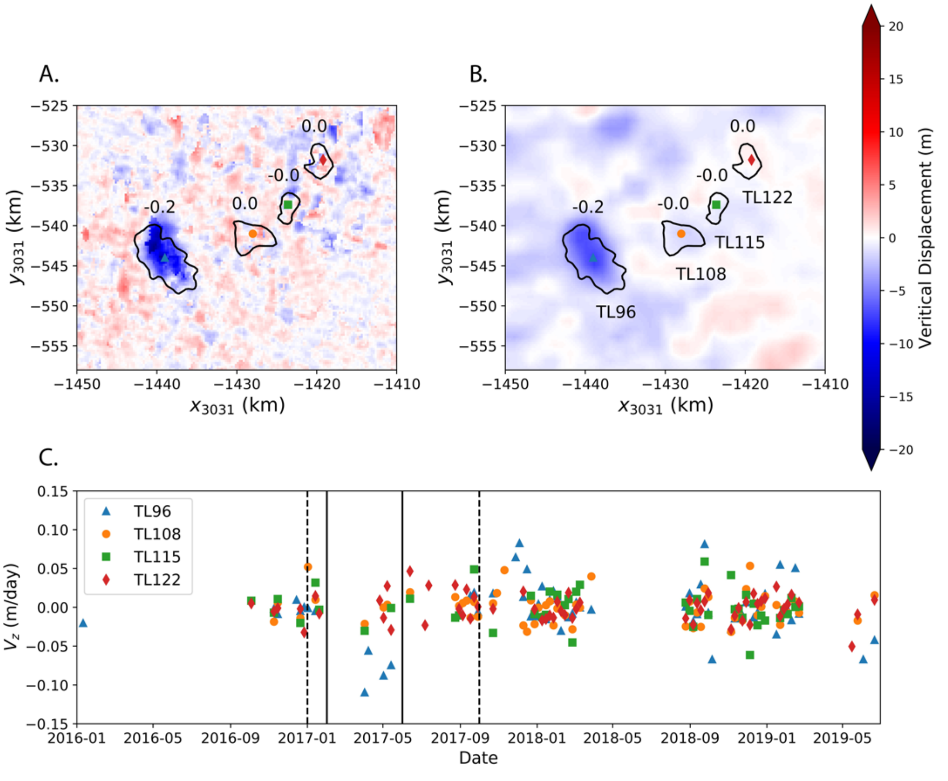

Supplement Figure 1: Surface elevation-change time series over the Haynes Glacier lakes showing the 2017 drainage event from (A) vertical displacement computed from integrated vertical displacement rates (V_z) from Sentinel-1 SAR data and (B) swath-processed radar altimetry in a polar stereographic projection (EPSG:3031). Water volume (km^3) associated with observed vertical displacement is labelled for each lake. (C) Time series of uplift rates (V_z) from SAR LOS results (coloured dots, left abscissa;

locations marked in panels A and B) and horizontal speed from GNSS observations (right abscissa). Solid lines represent period over which SAR vertical displacements (V_z) were integrated to produce the vertical displacements shown in panel A. Dotted lines represent the quarters of gridded CryoSat-2 data differenced to create panel B.

-

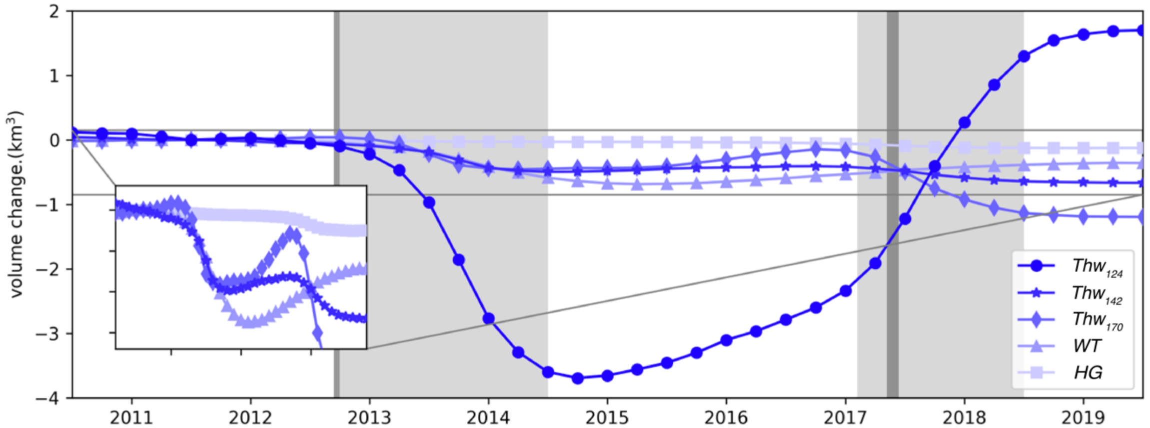

Supplement Figure 2: Volume change for all observed subglacial lakes over the complete observation period derived from CryoSat-2 data by subtracting an average thinning rate outside the lake from the average elevation change in the lake and multiplying by the lake area.

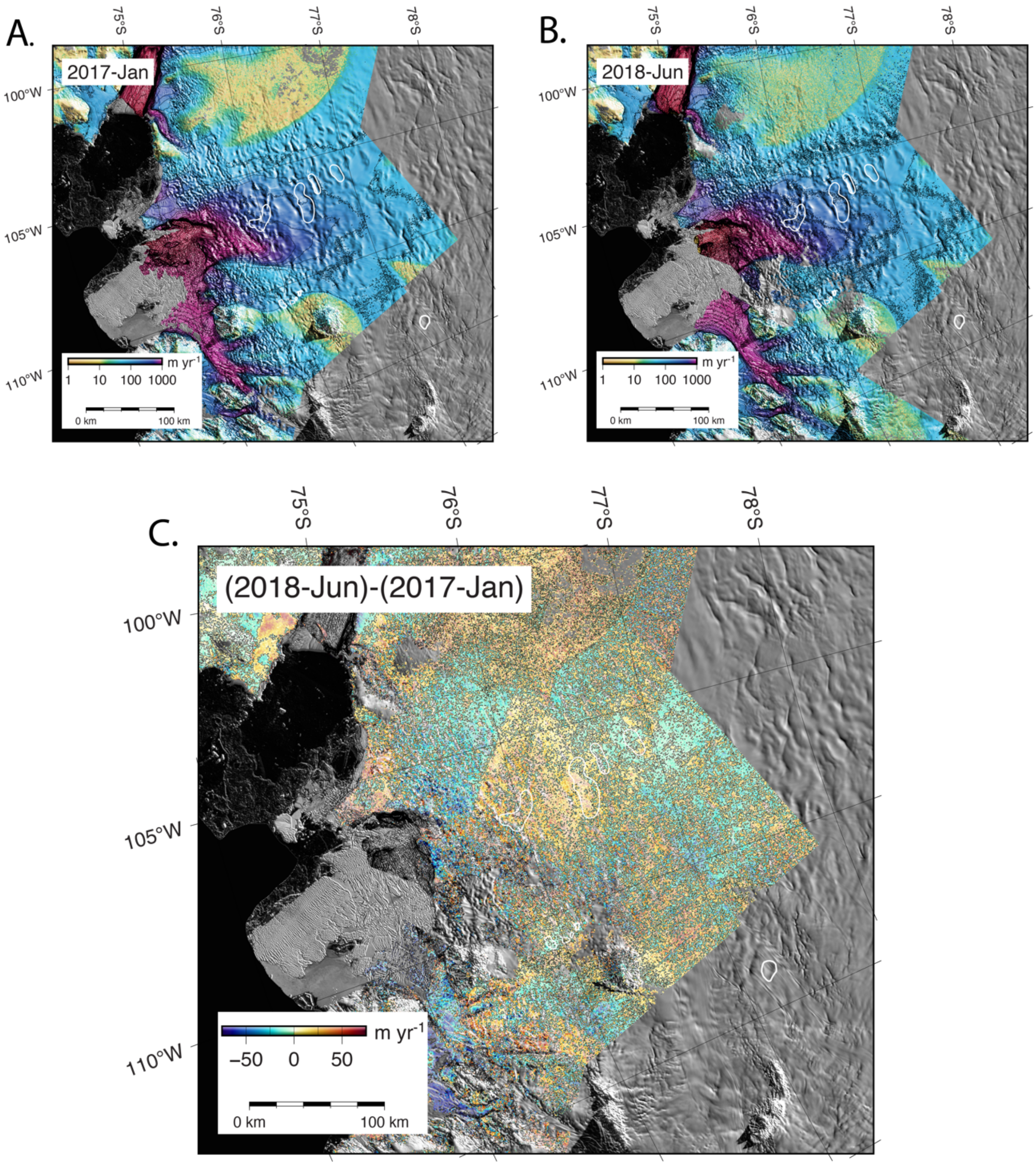

Supplement Figure 3: Distributed velocities from SAR image pairs with centre acquisition dates (A) 01/2017 and (B) 01/2018 with (C) velocity difference (01/2018- 01/2017). There are no detectable changes in velocity associated with the drainage of lakes Thw_{142} and Thw_{170} into lake Thw_{124} or the Haynes Glacier lake drainage.

3 Hydropotential, water routing, and lake volume change

From the CryoSat-2 elevation change time series, we construct quarterly models of glaciostatic hydraulic potential. We first calculate a reference elevation model associated with the drained lakes. In the lake polygons, anomalous height change relative to background thinning is linked to filling and draining of subglacial water. Following Shreve (1972), we estimate the glaciostatic hydropotential as

$$\phi_q = P_q + \rho_{water} g z$$

where the water pressure at each quarter, $\boldsymbol{P_q}$, is assumed to be near the sum of the overburden stress of ice and lake water thickness, $\boldsymbol{H_q}$ and $\boldsymbol{h_q}$, respectively:

$$P_q \cong \rho_{ice} g H_q + \rho_{ice} g h_q$$

We then derive subglacial water fluxes multiplying the flow accumulation associated with the hydraulic potential time series by the distributed basal-melt field derived by Joughin et al. (2009). We assume the melt rates are stationary relative to the ongoing thinning and derive water routing beneath Thwaites Glacier (S4; see supplement movie). The water routing between the lakes remains relatively constant, despite local elevation changes as the lakes fill and drain and a general increase the hydraulic potential difference between the lakes as the lower reaches of Thwaites Glacier thin.

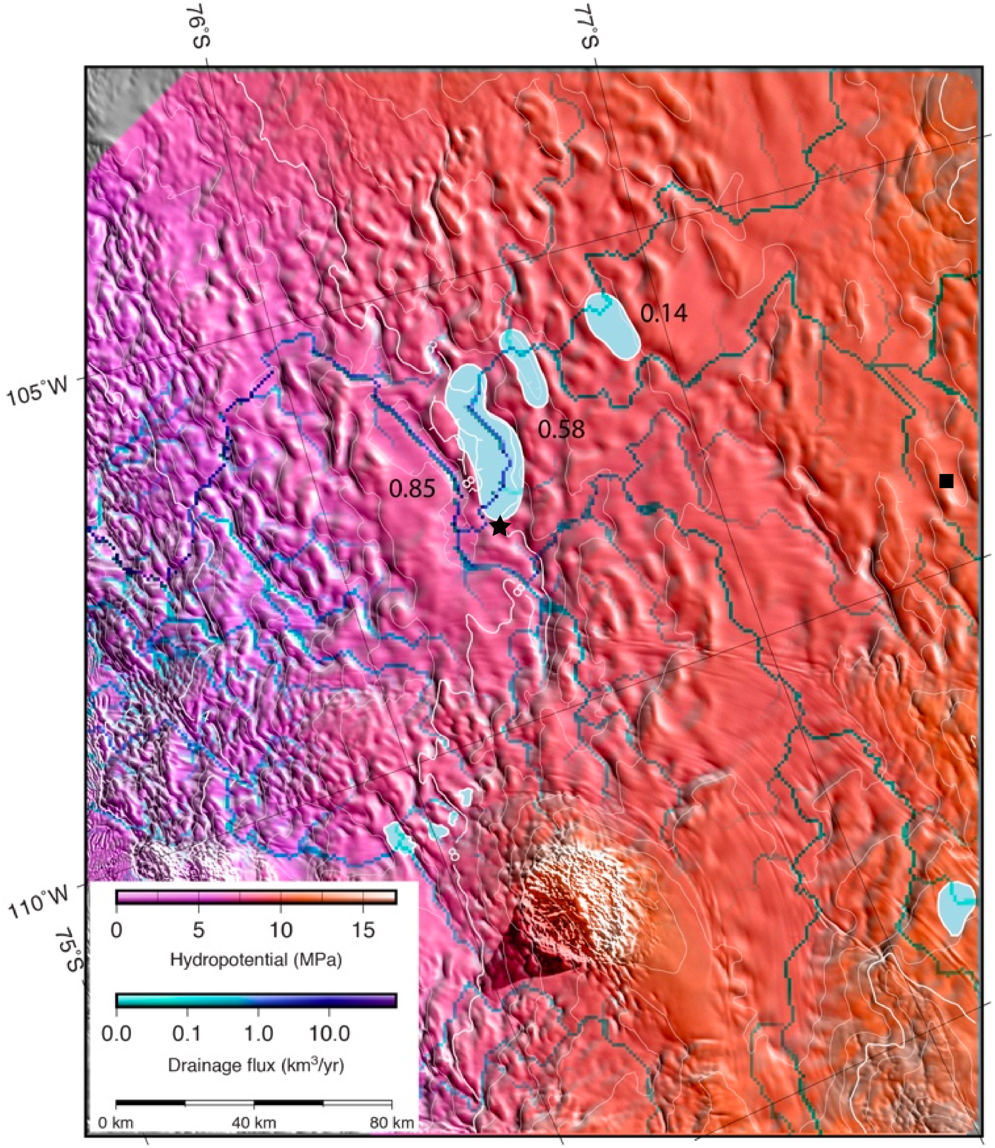

Supplement Figure 4: Average water flux assuming static hydropotential and basal-melt rates from Joughin et al. (2009). Supplement movie shows weak sensitivity for water rerouting as the glacier thins and the lakes fill and drain. The cumulative water fluxes (km^3/yr) into lakes $Thw_{124,142,170}$ are printed with each lake. Black star and square indicate sites of LTHW and UTHW GNSS.

4 Inversions of basal friction

Modelled ice temperature depends on the inferred basal shear stress and ice viscosity because of their combined effect on frictional and strain heating near the bed. Ice viscosity is best described by a temperature-dependent Arrhenius relation, which makes simultaneous inferences of ice rheology and basal friction difficult to separate from snap-shot observations of ice thickness and velocity. In our diagnostic inversions for bed friction and the enhancement factor, we use the ice-flow model icepack (doi:10.5281/zenodo.3542092) to solve the weak form of the shallow-shelf equations (Bueler et al., 2009), modified to include frictional energy dissipation:

$$F(u) = \int_{\Omega} \tau \left(\left(u_0^{\frac{1}{m}+1} + |u|^{\frac{1}{m}+1} \right)^{\frac{m}{m+1}} - u_0 \right) dx.$$

This functional describes the stress accommodation of the bed assuming a regularized Coulomb friction law (Joughin et al., 2019). We iteratively refine our proxies for bed resistance, $\tau = \tau_0 e^{\beta}$, and the fluidity in Glen's flow law, $A = A_0 e^{\theta}$, using the Gauss-Newton method to perturb parameters β and θ to minimize the objective functional:

$$E(u) = \int_{\Omega} \left(\frac{u - u_{obs}}{\sigma} \right)^2 dx,$$

where u are the modelled velocities and σ are the standard deviations of the measured SAR velocities, u_{obs}. In our iterative inversion scheme, we first calculate the depth-averaged enhancement factor from the 3D temperatures derived by Van Liefferinge and Pattyn (2013) and use this initial estimate to infer an initial basal shear stress field. For the floating eastern Thwaites Ice Shelf, where we do not have independently modelled ice temperatures, we assume a constant viscosity before advecting the initial temperature solution through the shelf (~20 years of spin up). We do not include the rifted western Thwaites Ice Shelf in our model domain because we find it provides almost no backstress to grounded ice, which is in agreement with previous work (Luchitta et al., 1993, Reese et al., 2017). Because almost all relative motion is accommodated by sliding in the shallow-shelf equations, our procedure overestimates shear stress at the ice-bed interface; however, our interest in differences between two representative model periods (before and after the lakes drain) makes this model assumption less impactful. Figure S5 shows the results of these simulations where deviations of shear stress inside the lake are smaller than outside the lake. This suggests that the lake fill-drain cycles have only minimal and/or temporary effects on ice dynamics both locally and for the broader basin.

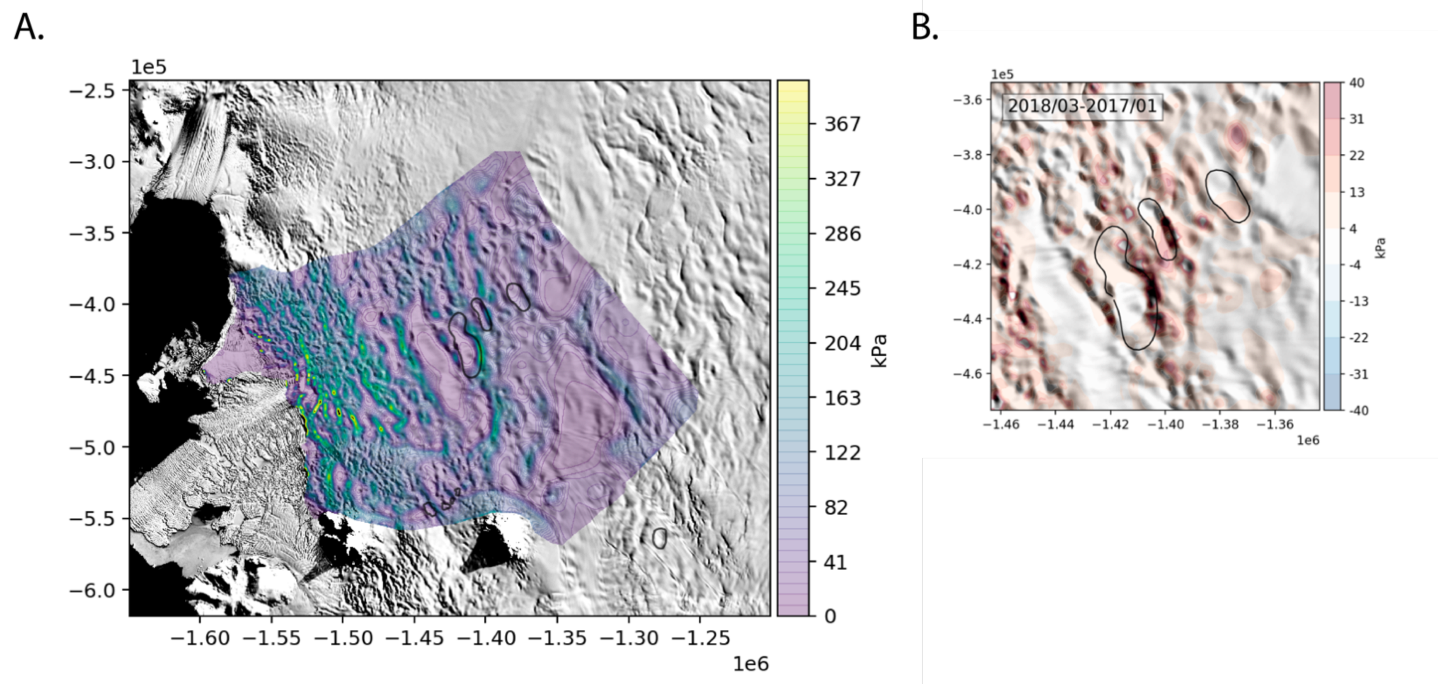

Supplement Figure 5: Static inversion for basal resistance field for 2017 catchment geometry (A) before the Haynes Glacier and Thwaites Glacier drainage events and (B) difference in inferred basal resistance between two static inversions from 2017 and 2018 (before and after the 2017 drainage cascade) for lakes $\mathbf{Thw_{124,142,170}}$.

References

Bueler E., Brown, J.: Shallow shelf approximation as a sliding law in a thermodynamically coupled ice sheet model, . J. Geophys. Res, 114, F1, 2009. doi:10.1029/2008JF001179.

Joughin, I., Tulaczyk, S., Bamber, J., Blankenship, D., Holt, J., Scambos, T., & Vaughan, D.: Basal conditions for Pine Island and Thwaites Glaciers, West Antarctica, determined using satellite and airborne data. Journal of Glaciology, *55*(190), 245-257, 2009. doi:10.3189/002214309788608705.

Joughin, I., Smith, B., and Schoof, C.: 2019. Regularized Coulomb Friction Laws for Ice Sheet Sliding: Application to Pine Island Glacier, Antarctica. Geophy Res. Lett., 46, 4764–4771. doi:10.1029/2019GL082526.

Lucchitta, B., Mullins, K, Allison, A., & Ferrigno, J. (1993). Antarctic glacier-tongue velocities from Landsat images: First results. Annals of Glaciology, 17, 356-366. doi:10.3189/S0260305500013100.

Reese R., Gudmundsson G.H., Levermann, A., Winkelmann, R.: The far reach of ice-shelf thinning in Antarctica, Nature Climate Change, 8, 53-57, 2018. doi:10.1038/s41558-017-0020-x.

Shreve, R. L.: Movement of water in glaciers, J. Glaciol., 11, 205– 214, 1972.

Van Liefferinge B., and Pattyn F., Using ice-flow models to evaluate potential sites of million-year-old ice in Antarctica, Clim. Past, 9, 2335-2345, 2013. doi:10.5194/cp-2335-2013.